transcription (*14*). To generate a muscle cell from nonmuscle tissue, fibrosarcoma cells may repress (or lose) these loci, resulting in the activation of *MyoD* transcription. Because MyoD can induce growth arrest (*15*), its expression in a fibrosarcoma may serve as a "fail-safe" mechanism to prevent cell growth. Additional genetic defects that prevent MyoD function, such as the recessive defects described here, would prevent differentiation and result in the generation of a rhabdomyosarcoma. A similar mechanism may apply to other types of tumors that express full or partial differentiation programs.

REFERENCES AND NOTES

1. H. Scrable *et al.*, *Genes Chromosomes Cancer* **1**, 23 (1989).
2. P. Dias *et al.*, *Am. J. Pathol.* **137**, 1283 (1990).
3. S. J. Tapscott and H. Weintraub, *J. Clin. Invest.* **87**, 1133 (1991); H. Weintraub *et al.*, *Science* **251**, 761 (1991); E. N. Olson, *Genes Dev.* **4**, 1454 (1990).
4. H. Weintraub *et al.*, *Proc. Natl. Acad. Sci. U.S.A.* **86**, 5434 (1989); J. Choi *et al.*, *ibid.* **87**, 7988 (1990).
5. The RD [R. M. McAllister, J. Melnyk, J. Z. Findelstein, E. C. Adams, Jr., M. B. Gardner, *Cancer (Phila.)* **24**, 520 (1969)] and Rh18 [B. J. Hazelton *et al.*, *Cancer Res.* **47**, 4501 (1987)] cell lines were established from embryonal rhabdomyosarcomas. Rh28, Rh30, and RhJT [E. C. Douglas *et al.*, *Cytogenet. Cell Genet.* **45**, 148 (1987); P. J. Houghton, personal communication] are cell lines established from alveolar rhabdomyosarcomas.
6. The *E2A* gene codes for *E12*, *E47*, and *E2-5* RNA (*3*).
7. Id is a negative regulator of MyoD [R. Benezra, R. L. Davis, D. Lockshon, D. L. Turner, H. Weintraub, *Cell* **61**, 49 (1990); J. Yale, H. Weintraub, R. Benezra, *Genes Dev.* **6**, 1466 (1992)].
8. S. J. Tapscott, M. J. Thayer, H. Weintraub, unpublished data.
9. R. L. Davis *et al.*, *Cell* **51**, 987 (1987).
10. A. L. Hiti *et al.*, *Mol. Cell. Biol.* **9**, 4722 (1989).
11. A. B. Lassar *et al.*, *Cell* **66**, 305 (1991).
12. H. Weintraub *et al.*, *Genes Dev.* **5**, 1377 (1991).
13. E. C. Douglas *et al.*, in (*5*).
14. M. J. Thayer and H. Weintraub, *Cell* **63**, 23 (1990).
15. V. Sorrentino *et al.*, *Nature* **345**, 813 (1990); M. Crescenzi *et al.*, *Proc. Natl. Acad. Sci. U.S.A.* **87**, 8442 (1990).
16. H. M. Blau, C.-P. Chiu, C. Webster, *Cell* **32**, 1171 (1983).
17. A. B. Lassar *et al.*, *ibid.* **58**, 823 (1989).
18. Cells were plated together in 6-cm tissue culture dishes, allowed to grow for 24 hours, and then rinsed with Dulbecco's minimum essential medium (DMEM, Sigma) at 37°C. Sterile 50% polyethylene glycol in DMEM was added for 1 min, and the cells were then washed four times with DMEM. Cells were fed again, with DMEM supplemented with 15% calf serum (Hyclone) for 24 hours, and switched to low-serum medium for 48 hours. For fixation, cells were treated with 4% paraformaldehyde in phosphate-buffered saline (pH 7.4) for 5 min at room temperature. Antisera for MyoD [S. J. Tapscott *et al.*, *Science* **242**, 405 (1988)] and MyHC [D. Bader, T. Masaki, D. A. Fischman, *J. Cell Biol.* **95**, 763 (1982)] have been described. The antiserum to CAT was obtained from 5-Prime 3-Prime (Boulder, CO).
19. All cells were grown in DMEM containing penicillin and streptomycin and supplemented with 15% calf serum (Supplemented Calf Serum, Hyclone). Transient transfections and CAT assays were performed as described in (*12*).

20. S.J.T. is a McDonnell Fellow in Molecular Medicine in Cancer Research and H.W. is a Howard Hughes Investigator. Supported by fellowship DRG-1000 of the Damon Runyon–Walter Winchell Cancer Fund (M.J.T.) and National Institutes of Health funds (M.J.T. and H.W.). We thank T. K. Blackwell for assistance in the early experiments, P. J. Houghton for rhabdomyosarcoma cell lines and valuable advice, and S. Hauschka for the antiserum to MCK. The project would not have been initiated without the forum provided by the First Robert Steel Foundation International Symposium.

3 August 1992; accepted 9 December 1992

Antagonism of Catecholamine Receptor Signaling by Expression of Cytoplasmic Domains of the Receptors

Louis M. Luttrell, Jacek Ostrowski,* Susanna Cotecchia,† Humphrey Kendall, Robert J. Lefkowitz‡

The actions of many hormones and neurotransmitters are mediated by the members of a superfamily of receptors coupled to heterotrimeric guanine nucleotide–binding proteins (G proteins). These receptors are characterized by a highly conserved topographical arrangement in which seven transmembrane domains are connected by intracellular and extracellular loops. The interaction between these receptors and G proteins is mediated in large part by the third intracellular loop of the receptor. Coexpression of the third intracellular loop of the α_{1B}-adrenergic receptor with its parent receptor inhibited receptor-mediated activation of phospholipase C. The inhibition extended to the closely related α_{1C}-adrenergic receptor subtype, but not the phospholipase C–coupled M1 muscarinic acetylcholine receptor nor the adenylate cyclase–coupled D_{1A} dopamine receptor. These results suggest that the receptor–G protein interface may represent a target for receptor antagonist drugs.

The binding of agonists to G protein–coupled receptors induces conformational changes in the receptor that promote formation of an agonist receptor–G protein ternary complex (*1*) that leads to G protein activation and productive coupling to the effector. The interaction between receptor and G protein is mediated by the intracellular loops of the receptor. Mutagenesis studies of the third intracellular (3i) loop of several G protein–coupled receptors indicate that this region is critical for productive coupling (*2*). Studies with chimeric adrenergic receptors (ARs) (*3*, *4*) and muscarinic cholinergic receptors (AChRs) (*5*) implicate the putative 3i loop as the major, but not the sole, determinant of selective coupling to their respective G proteins.

A large number of clinically important therapeutic agents are drugs that can occupy the ligand-binding pocket of G protein–coupled receptors without inducing receptor activation, also known as receptor antagonists. To date, virtually all known antagonists of such receptors share the common property of blocking access of the ligand to the receptor. We wondered whether an alternative strategy for designing receptor antagonists might be to block the interaction of the receptor itself with the G protein. Given the importance of the 3i loop of several G protein–coupled receptors in forming the site of contact between the receptor and G protein, we tested the feasibility of expressing this isolated region of the receptor in intact cells and its effects on receptor function. We report that coexpression of the 3i loop with its homologous receptor resulted in a specific antagonism of receptor-mediated signaling.

To determine the effects of the putative 3i loop of the α_{1B}-AR on basal and receptor-mediated second messenger production, we prepared minigene constructs (Fig. 1A) that encoded either the full 3i loop (residues 225 to 295) (α_{1B}-3i), its NH_2-terminal portion (residues 225 to 272) (α_{1B}-3iN), or its COOH-terminal portion (residues 273 to 295) (α_{1B}-3iC). The α_{1B}-3iN construct spans a 27–amino acid motif, residues 233 to 259, important in determining the selectivity of receptor–G protein coupling (*4*). The α_{1B}-3iC construct contains a 7–amino acid domain, residues 288 to 294, that influences the affinity of agonist binding and the potency of agonist-stimulated activation of phospholipase C (PLC) (*3*, *6*). Another minigene construct

Departments of Medicine and Biochemistry and the Howard Hughes Medical Institute, Duke University Medical Center, Durham, NC 27710.

*Present address: Bristol-Myers Squibb Pharmaceutical Research Institute, Buffalo, NY 14213.
†Present address: Institut de Pharmacologie et Toxicologie, Faculté de Médecine, 1005 Lausanne, Switzerland.
‡To whom correspondence should be addressed.

was prepared encoding the full 3i loop, residues 215 to 273 (D_{1A} 3i), of the D_{1A} dopamine receptor (*7*). For transient cellular expression, the minigene constructs were inserted into the expression vector pRK5 (*8*), generating the plasmids pRKα_{1B}3i, pRKα_{1B}3iN, pRKα_{1B}3iC, and pRKD_{1A}3i; the plasmid DNA was then transfected into 293 cells (human embryonal kidney). Cellular expression of the 8-kD α_{1B}-3i peptide was documented by protein immunoblotting of the peptide immunoprecipitated from whole cell lysates with an antiserum to α_{1B}-3i (Fig. 1B). The amount of peptide expression increased proportionately with the amount of plasmid DNA used in the transfection and was ~170 fmol per milligram of whole cell protein in cells transfected with 10 μg of pRKα_{1B}3i per dish of cells.

Untransfected 293 cells expressed little endogenous α_1-AR (<10 fmol per milligram of membrane protein) and no detectable epinephrine-stimulated inositol phosphate (IP) production. Cells transfected with pRKα_{1B}3i, pRKα_{1B}3iN, or pRKα_{1B}3iC exhibited no detectable intrinsic stimulation of IP production, as compared with cells transfected with equal amounts of pRK5 alone (*9*). To determine if expression of the α_{1B}-3i peptide had any effect on α_{1B}-AR–mediated activation of phosphatidylinositol (PI) hydrolysis, we cotransfected 293 cells with pRK5 containing cDNA encoding the α_{1B}-AR (pRKα_{1B}AR) and pRKα_{1B}3i. The amount of α_{1B}-AR expression increased with the amount of transfected receptor DNA to a maximum of 4 pmol per milligram of membrane protein. At any amount of receptor expression, cells cotransfected with pRKα_{1B}3i exhibited marked attenuation of epinephrine-stimulated IP production, as compared with cells cotransfected with pRK5 alone (Fig. 2A). The range of receptor expression obtained (0.05 to 4 pmol per milligram of membrane protein) corresponds to approximately 10 to 900 fmol per milligram of whole cell protein, similar to the estimated amount of α_{1B}-3i loop expression determined from protein immunoblots. The extent of α_{1B}-3i–mediated inhibition was dependent on the amount of pRKα_{1B}3i transfected and was maximal (70% inhibition of control response) in cells transfected with 15 μg of plasmid DNA per dish of cells (Fig. 2B).

To determine whether the capacity of the α_{1B}-3i loop to inhibit α_{1B}-AR–mediated PI hydrolysis was contained solely within the NH_2- or COOH-terminal regions of the peptide, we determined basal and epinephrine-stimulated IP production in cells cotransfected with pRKα_{1B}AR and either pRK5 alone, pRKα_{1B}3i, pRKα_{1B}3iN, or pRKα_{1B}3iC. None of the 3i loop–derived constructs produced a significant effect on α_{1B}-AR expression or basal IP production, as compared with pRK5 alone (Table 1). Whereas coexpression of the full α_{1B}-3i loop resulted in a 60% attenuation of epinephrine-stimulated IP production, cotransfection with either pRKα_{1B}3iN or pRKα_{1B}3iC did not produce significant inhibition. In contrast, simultaneous cotransfection of pRKα_{1B}3iN and pRKα_{1B}3iC with pRKα_{1B}AR resulted in a 44% inhibition, mimicking the effect of the intact α_{1B}-3i loop. These data suggest that epitopes from both the NH_2- and COOH-terminal domains of the 3i loop may be necessary to block productive receptor–G protein coupling. Alternatively, physical interaction between the two domains of the 3i loop may be necessary to impart the proper conformation to the domain that is critical for biological activity. The epinephrine concentration required for half-maximal stimulation of IP production was similar in all of the cotransfectants; the inhibition resulted from a decrease in the maximal response (Fig. 2C).

To define the specificity of the 3i loop–mediated antagonism, we assessed the effect of α_{1B}-3i loop expression on signal transduction through other G protein–coupled receptors, including the α_{1C}-AR, M1 muscarinic AChR, and D_{1A} dopamine receptor. The α_{1B}-AR stimulates PI hydrolysis catalyzed by PL-C by means of a pertussis toxin (PT)–insensitive G protein (*10*), probably a member of the G_q family (*11*). Coexpression of the α_{1B}-3i loop with the α_{1B}-AR attenuated receptor-mediated IP production (Fig. 3A). The α_{1C}-AR subtype is similar in amino acid

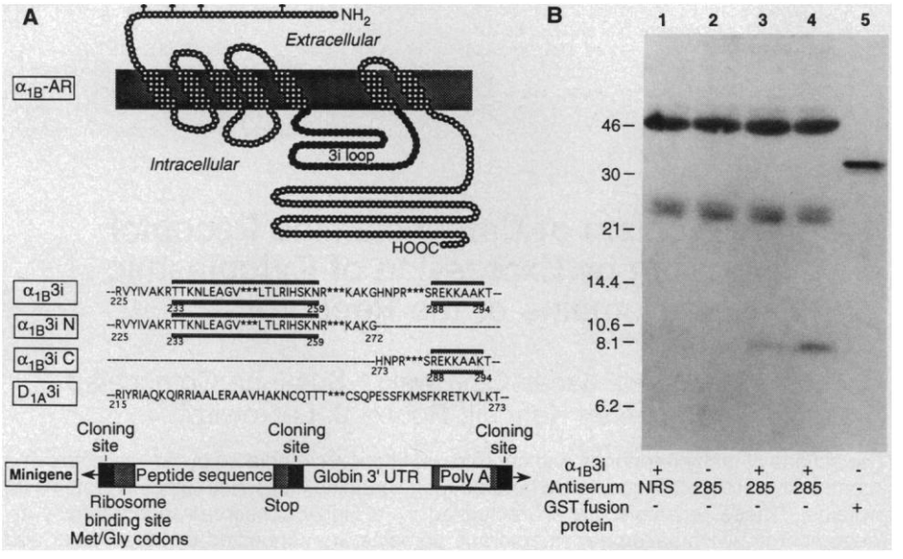

Fig. 1. Expression of the 3i loop of the α_{1B}-AR in 293 cells. (**A**) Construction of a minigene encoding α_{1B}-AR–derived peptides. The upper panel depicts the relative position of the 3i loop with respect to the putative membrane topography of the hamster α_{1B}-AR. The center panels show the amino acid sequences (*16*) of the hamster α_{1B}-AR and human D_{1A} receptor putative 3i loops used in each construct. Numbers refer to the amino acid positions within the receptor. Asterisks represent regions where the sequence is not shown. The areas bracketed by underlining and overlining indicate the positions of the 27–amino acid region in the NH_2-terminal portion and the 7–amino acid region in the COOH-terminal portion of the 3i loop. The DNA encoding each of the peptides shown was cloned into a minigene construct depicted schematically in the lower panel (*24*). (**B**) Protein immunoblot depicting the expression of the 3i loop of the α_{1B}-AR in 293 cells. Cells maintained in minimum essential medium supplemented with 10% fetal bovine serum and gentamicin (100 μg/ml) were plated in 100-mm dishes (2×10^6 cells per dish) and transfected by coprecipitation of DNA in calcium phosphate (*25*) with pRK5 alone (10 μg) (lane 2), pRKα_{1B}3i (1 μg) and pRK5 (9 μg) (lane 3), or pRKα_{1B}3i (10 μg) (lane 4). Forty-eight hours after transfection, whole cell detergent lysates containing ~6 mg of protein per milliliter were incubated with a 1:50 dilution of rabbit polyclonal antiserum 285. The antiserum was raised to a synthetic peptide [SNSKELTLRIHSKNFHEDTLSRC (*16*)] derived from the third cytoplasmic domain of the α_{1B}-AR and conjugated to keyhole limpet hemocyanin through the COOH-terminal cysteine. Immune complexes were collected on protein A–Sepharose (Pharmacia), washed, and denatured in Laemmli sample buffer. Immunoprecipitated peptide was resolved by SDS–polyacrylamide gel electrophoresis with the discontinuous procedure of Schägger and von Jagow (*26*) and then transferred to nitrocellulose. Filters were incubated in a 1:100 dilution of antiserum 285 and probed with ^{125}I-labeled protein A. Peptides were visualized by autoradiography. Amount of expression was estimated by phosphorimage densitometry with known amounts of a purified glutathione S-transferase (GST) fusion protein containing the full α_{1B}-3i (*27*) as standard. Cells transfected with pRKα_{1B}3i and immunoprecipitated with normal rabbit serum (NRS) (lane 1) and a purified GST fusion protein containing the full α_{1B}-3i (residues 225 to 295) (lane 5) were used as negative and positive controls, respectively. Molecular size standards are shown at the left (in kilodaltons).

sequence to the α_{1B}-AR (~72% identity in the presumed membrane-spanning domains) (*12*) and also couples to PL-C through a PT-insensitive G protein (*13*). The putative 3i loop of the α_{1C}-AR is similar in length to the α_{1B}-3i loop and shares ~52% identity with it, including 13 of 15 amino acids at the COOH-terminus of the loop. Coexpression of the α_{1B}-3i loop and α_{1C}-AR resulted in a 65% attenuation of α_{1C}-AR–mediated PI production (Fig. 3B), equal to that observed with the α_{1B}-AR. Thus, the two subtypes appear to share a common signal transduction pathway. At amounts of α_{1C}-AR expression between 0.1 and 6 pmol per milligram of membrane protein, inhibition by the 3i loop was statistically significant ($P < 0.02$; $n = 7$).

The M1 AChR, like the α_{1B}-AR and α_{1C}-AR, promotes PI hydrolysis through a PT-insensitive G protein. This activity can be reconstituted in phospholipid vesicles with purified M1 AChR and G_q or G_{11} (*14*). The putative 3i loop of the human M1 AChR is much larger than the α_{1B}-3i (*15*); however, 8 of 15 amino acids at the COOH-terminus of the putative 3i loop are common to both, including the sequence XEKKAAXT (*16*) just proximal to the sixth membrane-spanning domain. At amounts of M1 AChR receptor expression from 0.3 to 3 pmol per milligram of membrane protein, coexpression of the α_{1B}-3i loop resulted in a small but significant reduction in carbachol-stimulated PI hydrolysis ($P < 0.05$; $n = 8$) (Fig. 3C). If large amounts of receptor were expressed (>5 pmol per milligram of membrane protein), carbachol-stimulated PI hydrolysis was not inhibited. Neither α_{1B}-AR– nor M1 AChR–mediated PI production in transfected 293 cells was PT-sensitive (*9*).

The D_{1A} dopamine receptor stimulates adenylyl cyclase through the stimulatory G protein G_s (*17*). Despite this difference in G protein specificity, the putative 3i loop of the D_{1A} receptor shares significant homology at the COOH-terminus with the α_{1B}-AR and M1 AChR (*7*). To determine whether the α_{1B}-3i loop–mediated inhibition of signal transduction extended to G_s-coupled receptors, we determined the effect of α_{1B}-3i loop expression on activation of adenylyl cyclase by means of the D_{1A} receptor. Cotransfection of pRK5 containing the D_{1A} receptor cDNA (pRKD_{1A}R) with pRKα_{1B}3i had no effect on fenoldopam-stimulated production of adeno-

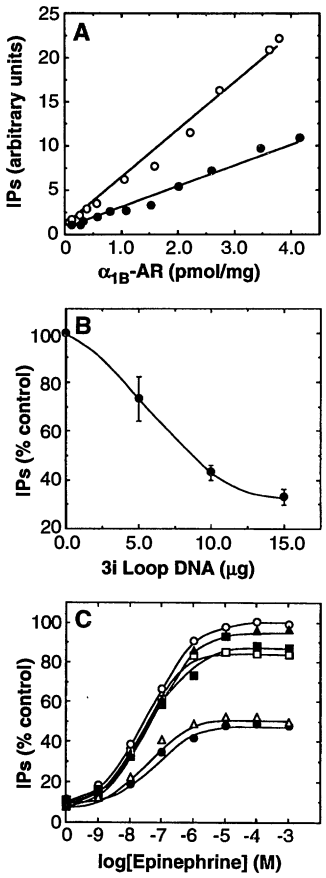

Fig. 2. Inhibition of α_{1B}-AR–mediated IP production by coexpression of the 3i loop of the receptor. (**A**) Effect of α_{1B}-3i loop expression on α_{1B}-AR–mediated IP production; 293 cells were cotransfected with pRKα_{1B}AR (0.1 to 5 μg per dish) and pRK5 (○) or pRKα_{1B}3i (●) (10 μg per dish). After transfection, cells were split for determination of ligand binding and IP production and assayed after 48 hours. We performed saturation binding of 1 nM [^{125}I]HEAT as described (*4*) using 1 μM prazosin to determine nonspecific binding. Binding data were normalized per milligram of membrane protein. Nonspecific binding was less than 10% of the total. IP production was determined in intact monolayers of transfected cells stimulated for 45 min with or without epinephrine (10 μM) as described (*4*). Data are presented in arbitrary units such that 1 unit is the basal amount of IP produced in the absence of epinephrine. Each point represents the mean of triplicate determinations performed on an independent transfection. Replicates varied by <10% of the means. (**B**) Effect of increasing amounts of pRKα_{1B}3i DNA on α_{1B}-AR–mediated IP production. Cells were cotransfected with pRKα_{1B}AR (1 μg per dish) and various amounts of pRKα_{1B}3i (●). The total amount of plasmid DNA per transfection was kept constant by the addition of pRK5. Expression of α_{1B}-AR was ~1 pmol/mg and varied <10% between transfections. Data were normalized to the amount of epinephrine-stimulated IP production observed in cells transfected with pRKα_{1B}AR and pRK5 (control). Each point represents the mean ± SEM for three separate experiments performed in triplicate. (**C**) Effect of epinephrine on IP production. Cells were cotransfected with pRKα_{1B}AR (1 μg per dish) and either pRK5 (○), pRKα_{1B}3i (●), pRKα_{1B}3iN (□), pRKα_{1B}3iC (■), pRKα_{1B}3iN plus pRKα_{1B}3iC (△), or pRKD_{1A}3i (▲) (10 μg per dish) and stimulated as described (*4*) with the indicated concentration of epinephrine. Data were normalized to the maximum response observed in cells transfected with pRKα_{1B}AR plus pRK5 in each experiment (control). Each curve represents the mean of three to six separate experiments performed in triplicate. Standard errors were <10% of the means.

Table 1. Parameters of ligand binding and activation of PI hydrolysis in 293 cells cotransfected with the α_{1B}-AR and 3i loop constructs. Cells were transiently cotransfected with pRKα_{1B}AR (1 μg per dish) and the indicated 3i loop construct (10 μg per dish). Saturation binding (B_{max}) of 2-[β-(4-hydroxy-3-[^{125}I]iodophenyl)ethylaminomethyl] tetralone ([^{125}I]HEAT) (*4*) and basal and epinephrine-stimulated IP production were determined as described (*4*). R_{basal} represents the amount of basal IP in arbitrary units such that 1 unit is the basal amount of IP produced in cells transfected with α_{1B}-AR and pRK5. R_{max} represents the epinephrine-stimulated (10 μM) increase in generation of IPs in arbitrary units such that 1 unit is the basal amount of IP produced under each set of cotransfection conditions. EC_{50} represents the concentration of epinephrine required for half-maximal stimulation of PI hydrolysis. Statistical significance was assessed with the Student's paired *t* test.

Plasmid	3i loop residues	Ligand binding [^{125}I]HEAT	IP production			
			Basal	Epinephrine		
		B_{max} (pmol/mg)*	R_{basal} (arbitrary units)*	R_{max} (arbitrary units)*	EC_{50} (nM)†	Inhibition of R_{max} (%)
pRK5		2.59 ± 0.43	1.00	11.5 ± 2.5	44.8	0.0
pRKα_{1B}3i	225–295	2.65 ± 0.43	1.05 ± 0.14	4.6 ± 0.6‡	43.6	60.0
pRKα_{1B}3iN	225–272	2.72 ± 0.57	1.00 ± 0.09	9.9 ± 2.6§	30.4	13.9
pRKα_{1B}3iC	273–295	2.72 ± 0.55	0.97 ± 0.12	11.4 ± 2.8§	47.7	0.9
pRKα_{1B}3iN + pRKα_{1B}3iC	225–272 + 273–295	2.58 ± 0.44	0.90 ± 0.08	6.5 ± 1.5‡	33.9	43.5
pRKD_{1A}3i	215–273	3.04 ± 0.66	0.98 ± 0.01	11.0 ± 2.0§	42.9	4.3

*Mean ± SEM of four to six separate triplicate determinations. †Mean of three to six separate triplicate experiments that agreed within 20%. ‡As compared with pRK5; $P < 0.02$. §Not significantly different from vector alone; $P > 0.10$.

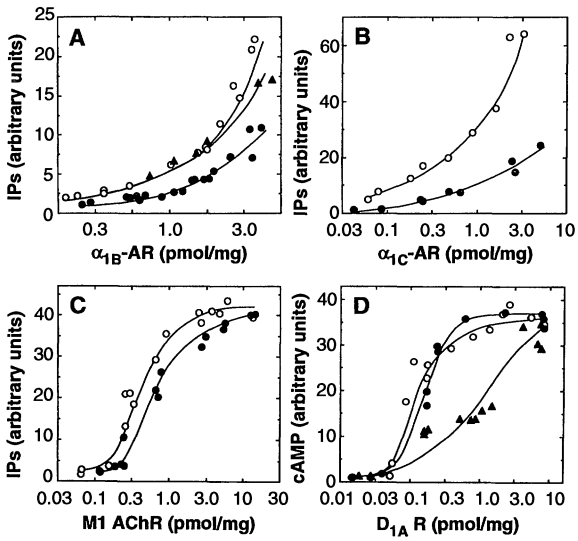

Fig. 3. Specificity of the 3i loop–induced inhibition of IP and cAMP production in 293 cells. (**A**) Effects of the α_{1B}-3i and D_{1A} 3i loops on α_{1B}-AR–mediated IP production. Cells were cotransfected with pRKα_{1B}AR (0.1 to 5 μg per dish) and pRK5 (○), pRKα_{1B}3i (●), or pRKD_{1A}3i (▲) (10 μg per dish). Expression of α_{1B}-AR– and epinephrine-stimulated IP production were determined as described (*4*). (**B**) Effect of the α_{1B}-3i loop on α_{1C}-AR–mediated IP production. Cells were cotransfected with pRKα_{1C}AR (0.01 to 5 μg per dish) and pRK5 (○) or pRKα_{1B}3i (●) (10 μg per dish). Expression of α_{1C}-AR– and epinephrine-stimulated IP production were determined as described (*4*). (**C**) Effect of the α_{1B}-3i loop on M1 AChR–mediated IP production. Cells were cotransfected with pRK5 containing the M1 AChR cDNA (0.01 to 5 μg per dish) and pRK5 (○) or pRKα_{1B}3i (●) (10 μg per dish). We determined M1 AChR expression by ligand binding of a saturating concentration of L-[benzilic-4,4′-^{3}H(*N*)]-quinuclidinyl benzilate (1 nM) to plasma membranes of transfected cells using 10 μM atropine to determine nonspecific binding under incubation conditions identical to those used for α_1-AR binding (*4*). Carbachol-stimulated (10 μM) IP production was determined as described (*4*). (**D**) Effects of the α_{1B}-3i and D_{1A} 3i loops on D_{1A} dopamine receptor–mediated cAMP production. Cells were cotransfected with pRKD_{1A}R (0.01 to 5 μg per dish) and either pRK5 (○), pRKα_{1B}3i (●), or pRKD_{1A}3i (▲) (10 μg per dish). We measured D_{1A} receptor (D_{1A} R) expression by ligand binding of a saturating concentration of the dopamine antagonist [^{3}H]SCH 23390 (New England Nuclear) (1 nM) to plasma membranes using *cis*-flupentixol (1 μM) to determine nonspecific binding, under incubation conditions identical to those used for α_{1B}-AR binding (*4*). Basal and fenoldopam (SKF 82526, SmithKline and Beecham)–stimulated (10 μM) production of cAMP were determined as described (*28*). In all panels, IP production is presented in arbitrary units such that 1 unit is the basal amount of IP produced in unstimulated cells. Each point represents the mean of triplicate determinations performed on an independent transfection. Replicates varied by 10% of the means.

sine 3′,5′-monophosphate (cAMP) at any amount of receptor expression up to 7 pmol per milligram of membrane protein (Fig. 3D). In contrast, cotransfection of pRKDα_{1A}R with its own 3i loop construct pRKDα_{1A}3i resulted in a significant reduction in receptor-mediated cAMP production at amounts of receptor expression between 0.1 and 2 pmol per milligram of membrane protein ($P < 0.01$; $n = 7$). At higher receptor density (>5 pmol per milligram of membrane protein), this inhibitory effect was no longer detectable, indicating that the inhibition could be surmounted by an increase in receptor density. In analogous experiments, cotransfection of pRKα_{1B}AR with pRKD_{1A}3i produced no effect on epinephrine-stimulated IP production (Figs. 2C and 3A), indicating that the D_{1A} 3i loop–mediated inhibition was also G protein–specific.

These data suggest that cellular expression of the 3i loop of both the α_{1B}-AR and D_{1A} receptor results in specific receptor antagonism by impairing protein interaction at the receptor–G protein interface. This could occur by several mechanisms, such as by competition for G_α subunits between the hormone-receptor complex and the free 3i loop of the receptor. If this were the case, the inhibition should be surmountable by an increase in receptor density, thereby permitting the formation of more hormone-receptor complexes to compete with the 3i loop. The observation that the D_{1A} 3i loop–induced inhibition of D_{1A} receptor–stimulated cAMP production was not detected at high amounts of receptor expression supports this model, as does the failure of the α_{1B}-3i loop to inhibit carbachol-stimulated IP production in cells expressing large amounts of M1 AChR. In contrast, the α_{1B}-3i loop–induced inhibition of α_{1B}-AR– and α_{1C}-AR–stimulated PI hydrolysis was detected at all obtainable amounts of receptor expression. However, this may simply reflect an inability to achieve sufficient receptor density in these experiments.

If the 3i loop peptide competes for a portion of the receptor binding site on the G_α subunit, we would expect the antagonism to be G_α subunit specific so that any receptor that uses a common G_α subunit would be affected. However, our data indicate that α_{1B}-3i loop peptide is more effective in blocking α_{1B}-AR– and α_{1C}-AR–G protein interactions than it is in blocking M1 AChR–G protein interactions, even though all are apparently mediated through the same PT-insensitive G protein (*11, 14, 18*). These differences may be due to several factors, including the following: (i) heterogeneity in the G_α subunits involved with the coupling of the α_{1B}-AR versus those involved with the M1 AChR; (ii) stabilization of the hormone–M1 AChR–G protein interaction through the involvement of other intracellular regions of the receptor; or (iii) greater interaction between M1 AChR and G protein in the absence of agonist (for example, precoupling), resulting in a decreased interaction between the 3i loop peptide and G_α subunit.

Alternatively, a different mechanism may be involved, such as an interaction between the 3i loop peptide and the intracellular domains of the parent receptor, thus producing a more receptor-specific inhibition of G protein activation. Such interactions might mimic intramolecular interactions that normally serve to keep the unliganded receptor in its constrained or inactive conformation, or they might disrupt receptor conformation in other ways.

Peptides derived from the COOH-terminal region of the β_2-AR 3i loop (*19*), the COOH-terminal region of the M4 AChR 3i loop, and the COOH-terminal region of the α_2-AR-C10 3i loop (*20*) mimic receptor by activating G proteins in vitro. Peptides derived from the COOH-terminal region of the 3i loop of the α_2-AR inhibit receptor–G protein interaction in membrane preparations (*21*), as do peptides derived from the 2i, 3i, and 4i domains of rhodopsin (*22*). An oligopeptide substance P analog has been shown to competitively antagonize receptor-mediated activation of G_i, G_o, and G_s in phospholipid vesicles by binding to G_α subunits (*23*). Our data demonstrate that peptides derived from the 3i loop of G protein–coupled receptors produce G protein–specific inhibition of receptor-mediated biological effects in the intact cell. This form of receptor antagonism might provide a model for the development of a class of receptor antagonists that specifically blocks signal transduction at the level of the receptor–G protein interaction.

REFERENCES AND NOTES

1. A. De Lean *et al.*, *J. Biol. Chem.* **255**, 7108 (1980); M. E. Maguire *et al.*, *Adv. Cyclic Nucleotide Res.* **8**, 1 (1977); R. S. Kent *et al.*, *Mol. Pharmacol.* **17**, 14 (1980).
2. C. D. Strader *et al.*, *J. Biol. Chem.* **262**, 16439 (1987); B. F. O'Dowd *et al.*, *ibid.* **263**, 15985 (1988); R. A. Dixon *et al.*, *Cold Spring Harbor Symp. Quant. Biol.* **53**, 487 (1988); R. R. Franke, B. König, T. P. Sakmar, H. G. Khorana, K. P. Hofmann, *Science* **250**, 123 (1990).
3. S. Cotecchia, S. Exum, M. G. Caron, R. J. Lefkowitz, *Proc. Natl. Acad. Sci. U.S.A.* **87**, 2896 (1990).
4. S. Cotecchia *et al.*, *J. Biol. Chem.* **267**, 1633 (1992).
5. T. Kubo *et al.*, *FEBS Lett.* **241**, 119 (1988).
6. M. A. Kjelsberg *et al.*, *J. Biol. Chem.* **267**, 1430 (1992).
7. A. Dearry *et al.*, *Nature* **347**, 72 (1990).
8. D. L Eaton *et al.*, *Biochemistry* **25**, 8343 (1986).
9. L. M. Luttrell, unpublished data.

10. S. Cotecchia *et al.*, *Proc. Natl. Acad. Sci. U.S.A.* **85**, 7159 (1988); C. J. Lynch *et al.*, *Mol. Pharmacol.* **29**, 196 (1986).
11. D. Wu, A. Katz, C.-H. Lee, M. I. Simon, *J. Biol. Chem.*, in press; S. Cotecchia, unpublished data.
12. D. A. Schwinn *et al.*, *J. Biol. Chem.* **265**, 8183 (1990).
13. D. A. Schwinn *et al.*, *Mol. Pharmacol.* **40**, 619 (1991).
14. G. Berstein *et al.*, *J. Biol. Chem.* **267**, 8081 (1992).
15. E. G. Peralta *et al.*, *EMBO J.* **6**, 3923 (1987).
16. Abbreviations for the amino acid residues are as follows: A, Ala; C, Cys; D, Asp; E, Glu; F, Phe; G, Gly; H, His; I, Ile; K, Lys; L, Leu; M, Met; N, Asn; P, Pro; Q, Gln; R, Arg; S, Ser; T, Thr; V, Val; W, Trp; X, a basic amino acid; and Y, Tyr.
17. J. Kebabian and D. Caine, *Nature* **277**, 93 (1979).
18. B. R. Conklin *et al.*, *J. Biol. Chem.* **267**, 31 (1992).
19. A. H. Cheung, C. H. Ruey-Ruey, M. P. Graziano, C. D. Strader, *FEBS Lett.* **279**, 277 (1991); T. Okamoto *et al.*, *Cell* **67**, 723 (1991).
20. T. Okamoto and I. Nishimoto, *J. Biol. Chem.* **267**, 8342 (1992).
21. H. M. Dalman and R. R. Neubig, *ibid.* **266**, 11025 (1991).
22. B. König *et al.*, *Proc. Natl. Acad. Sci. U.S.A.* **86**, 6878 (1989).
23. H. Mukai, E. Munekata, T. Higashijima, *J. Biol. Chem.* **267**, 16237 (1992).
24. We used the polymerase chain reaction (PCR) to construct a set of minigenes containing fragments derived from the 3i loop of the α_{1B}-AR or D_{1A}-dopamine receptor spliced with the 3′-untranslated region (3′-UTR) of the human β-globin gene. We added the β-globin gene 3′-UTR to enhance the stability of mRNA. Each minigene contained a restriction site at the 5′ end for subcloning, followed by the ribosome-binding site consensus sequence GCCGCCACCATGG [M. Kozak, *J. Cell Biol.* **108**, 229 (1989)]. In all constructs, a methionine codon was added upstream from the receptor-specific sequences as a translation initiation site and was followed by a glycine codon (GGA). We chose glycine as the second amino acid to protect the consensus sequence for ribosome binding during translation and to protect the nascent polypeptide against proteolytic degradation. At the end of the α_{1B}-3i, α_{1B}-3iN, or α_{1B}-3iC coding segment, a TAA stop codon was added, followed by a restriction site and the β-globin gene 3′-UTR. At the 3′ end of each construct, restriction sites were engineered for subcloning. The D_{1A} 3i minigene construct was similarly prepared. All restriction sites and signaling sequences and the splice site between the 3i loop coding region and the β-globin gene 3′-UTR were introduced by synthetic oligonucleotides during PCR amplification. Oligonucleotides were synthesized on a DNA synthesizer (model 380A; Applied Biosystems). Amplification of DNA fragments was performed as described [R. M. Horton, R. D. Hunt, S. N. Ho, J. K. Pullen, L. R. Pease, *Gene* **77**, 61 (1989)]. Splicing reactions at strictly defined points between the peptide coding regions and the β-globin gene 3′-UTR were done with a modification of the general polymerase-mediated recombination protocol [R. K. Saika *et al.*, *Science* **239**, 487 (1988)], as described (*4*). After PCR amplification, the full-length minigene DNA fragments were cloned by standard methods into the eukaryotic expression vector pRK5.
25. J. R. Didsbury *et al.*, *Proc. Natl. Acad. Sci. U.S.A.* **88**, 11564 (1991).
26. H. Schägger and G. von Jagow, *Anal. Biochem.* **166**, 368 (1987).
27. D. B. Smith and K. S. Johnson, *Gene* **67**, 31 (1988).
28. Y. Salomon, *Methods Enzymol.* **195**, 22 (1991).
29. We thank E. G. Peralta for providing the cDNA for the human M1 AChR; T. Kurose for providing the α_{1B}-3i loop glutathione S-transferase fusion protein; Q. Ren for assistance in preparing DNA constructs; and M. G. Caron for providing the cDNA for the D_{1A} dopamine receptor, for discussions, and for critical reading of this manuscript. Supported in part by NIH grant HL16037.

4 September 1992; accepted 23 November 1992

T_H1 and T_H2 Cell Antigen Receptors in Experimental Leishmaniasis

Steven L. Reiner, Zhi-En Wang, Farah Hatam, Phillip Scott, Richard M. Locksley*

The complexity and chronicity of parasitic infections have obscured the identification of biologically relevant antigens. Analysis of the T cell receptor repertoire used by mice infected with *Leishmania major* revealed the expansion of a restricted population of CD4$^+$ cells. These cells expressed the V_α8-J_αTA72,V_β4 heterodimer in both progressive infection and protective immunity and across several major histocompatibility haplotypes. Thus, the same immunodominant parasite epitope drives the disparate outcomes of this infectious process, suggesting that candidate vaccine antigens selected by screening of immune individuals may be capable of exacerbating disease in genetically susceptible individuals.

A number of infections, including leprosy, leishmaniasis, and tuberculosis, have polarized manifestations that range from asymptomatic seroconversion to disseminated disease. Infection of BALB/c mice with *L. major* leads to parasitization of macrophages and progressive disease that closely mimics human visceral leishmaniasis, or kala-azar. Disease has been associated with expansion of the T helper 2 (T_H2) CD4$^+$ population. These cells contain transcripts for interleukin-4 (IL-4) and IL-10 (*1*), cytokines that interfere with the activation of infected macrophages to a leishmanicidal state (*2*). Several immunologic manipulations, including transient CD4$^+$ depletion (*3*) or administration of antibody to IL-4 (*4*), permit these animals to establish a healer phenotype comparable to genetically resistant mouse strains such as C57BL/6 and C3H/HeN. This phenotype has been associated with expansion of T_H1 CD4$^+$ cells that contain transcripts for interferon-γ (IFN-γ) (*1*, *4*). Transferred CD4$^+$ cell lines of the T_H1 or T_H2 type are capable of establishing a healer or nonhealer phenotype, respectively, in a manner dependent on the elaboration of one of two key cytokines, IFN-γ or IL-4 (*5*). Administration of neutralizing antibodies to IFN-γ or IL-4 can reverse a healer or nonhealer phenotype, respectively, but such interventions must occur close to the time of infection (*4*, *6*). Although leishmaniasis, like most parasitic infections, is a chronic disease, these experiments implicate early events in determining the critical CD4$^+$ T cell response that mediates the eventual outcome. To define the relation between parasite antigens capable of eliciting protective or nonprotective immune responses in a characterized model, we analyzed T cell receptor (TCR) usage at early time points.

The expansion of CD4$^+$ T cells in BALB/c mice (nonhealer phenotype), BALB/c mice induced to heal by treatment with antibody to IL-4 (anti–IL-4), and in C57BL/6 mice (healer phenotype) was characterized by monoclonal antibodies (MAbs) to most of the variable regions of TCRβ molecules. MAbs to four TCRα chains were also analyzed (Fig. 1). As measured by flow cytofluorometric analysis, few differences were evident between animals that cleared the infection and those that developed disease or between different major histocompatibility (MHC) haplotypes (BALB/c mice are *H-2^d* and C57BL/6 mice are *H-2^b*). V_β4-bearing CD4$^+$ cells were expanded three to four times in all experimental groups. Among the V_α families analyzed, V_α8 was also increased four to seven times by 2 weeks after inoculation of the parasite.

To assess TCR usage among parasite-specific T helper cells, we established 16 consecutive *Leishmania*-specific T_H2 clones (*7*) from six animals with progressive infection and cloned and sequenced the TCRs (Table 1). A strong bias toward V_α8 (50% of clones) and V_β4 (31%) usage was apparent: in three of the clones these gene products were paired and more than half of the $V_\alpha8^+$ T_H2 clones paired with J_αTA72 and had identical junctional nucleotide sequences. The pairings of V_β4 with J_β gene products were more diverse.

Three *L. major*–specific T_H1 clones were established from mice induced to heal after treatment with anti-CD4. An additional T_H1 clone, 9.1-2, which was established from a BALB/c mouse immunized by intravenous injection of parasite antigens, confers protection after adoptive transfer (*8*). Three of these four clones, including 9.1-2, contained the identical V_α8-J_αTA72 sequence found in several of the T_H2 clones. Two of these three clones used the V_β4-

S. L. Reiner, Z-E. Wang, F. Hatam, R. M. Locksley, Department of Medicine and Department of Microbiology and Immunology, University of California, San Francisco, San Francisco, CA 94143.
P. Scott, Department of Pathobiology, University of Pennsylvania, School of Veterinary Medicine, Philadelphia, PA 19104.

*To whom correspondence should be addressed.